21

Noise Reduction in Butterfly Valve Cavitation by Semicircular Fins and Visualization of Cavitation Flow

Kazuhiko Ogawa
Osaka Sangyo University,
Japan

1. Introduction

Butterfly valves have the advantage of being very compact and simple to install compared with other types of valves, and so they are widely used in industry. However, depending on the conditions, cavitation may occur around a butterfly valve. When severe noise and vibration occur because of cavitation around a butterfly valve, the valve body and pipe wall are subjected to erosion.

Butterfly valves are sometimes used inside the piping of air-conditioning facilities and the noise and vibration caused by cavitation can, in addition to making users uncomfortable, be mistaken for mechanical trouble. The need to prevent such noise and vibration is increasing from an environmental standpoint, and the prevention or suppression of cavitation itself is very important. Accordingly, many products have been proposed to prevent or control cavitation around many types of valves (Baumann,1991; Tullis,1989). As for research on the prevention of cavitation, the characteristics of a control valve with tortuous paths and an orifice with a multi-perforated cone to prevent cavitation from occurring around the orifice were reported.(Rahmaeyer et al.,1995; Kugou,1996)

These methods have already been applied to actual products, and those products have proved very successful in reducing noise. However, tortuous path valves, for example, are applicable only to cases wherein the fluids are clean and the shapes of the piping arrangements around the valves are complicated. Moreover, the air injection method that is very effective in reducing cavitation is limited to cases wherein the effect of air can be ignored. Hence, the authors proposed the sudden enlargement of a pipe downstream of a butterfly valve (Ogawa & Uchida,2005). This method was much simpler than the conventional methods. However, the sudden enlargement of the pipe is not adequate for flows containing particles because the particles accumulate in the enlarged section of the pipe.

The author has already proposed the attachment of fins to the valve body in order to further reduce cavitation noise around the butterfly valve (Ogawa & Uchida,2005, Ogawa,2008). This method can be used for flows containing particles because of the simple shape of the valve body. Cavitation occurs intensely around the butterfly valve because of the interference of the flow from the nozzle side with the flow from the orifice side (Itoh et

al.,1988). To avoid this interference, semicircular fins were attached to the valve body. In this paper, it was confirmed based on the experimental results that the attachment of the fins was very effective in reducing cavitation noise.

In this study, cavitation bubbles were photographed by Hi-speed camera and the size and number were measured from those photographs and the effect of the fins and the upstream velocity distribution were investigated. In past studies, photographs focusing on the aspect of the butterfly valve cavitation have been reported in great numbers. For example, it was pointed out that the most erosive cavitation around a butterfly valve is the vortex cavitation on the orifice side by means of the pressure-sensitive films and high speed photography (Tani et al,1991). An observation of butterfly valve cavitation and the measurement of cavitation noise were performed to diagnose the cavitation condition (Kimura and Ogawa, 1986). However, since the measurements of number and size of the cavitation bubbles were not carried out, the details of the cavitation growth were not clear. In this study, close-up photographs of cavitation bubbles were taken and their number and size were analyzed. The difference between the normal valve and the valve with the fins is reported in the following.

In actual piping arrangements, straight lengths in front of butterfly valves are not sufficient to obtain normal velocity distribution in many cases. In extreme cases, more than two valves are installed in series or bends are installed just ahead of or behind those valves. Under such conditions, the upstream velocity distribution is different from the usual turbulent velocity distribution. Therefore, under the condition that the velocity distribution is biased, confirmation of whether or not the attachment of fins is useful for the noise reduction is necessary.

2. Reduction of cavitation noise by using fins

Figure 1 shows a typical case of intense cavitation. A butterfly valve is not usually used under such conditions, but this cavitation appears when a valve repeatedly opens and closes. The separation of the flow and the vortex region around the butterfly valve during light or moderate cavitation is easily presumed in this case.

In Fig. 1, the upstream side appears on the left. The leading edge of the butterfly valve is on the upper left and the trailing edge (nozzle side) is on the lower right. The flow from the lower left region (nozzle side) of this photograph passes along the wall surface and interferes intensely with the flow from the upper left (orifice side) at the top of the pipe. It has been pointed out (Itoh et al.,1988) that this interference from both flows causes intense cavitation and brings about the erosion of the wall surface. Therefore, the fins were attached to the valve body in this study to avoid the interference caused by these flows. The interference of the flows and the separation of the flow behind the valve were expected to be reduced when the fins were attached to the downstream surface of the valve.

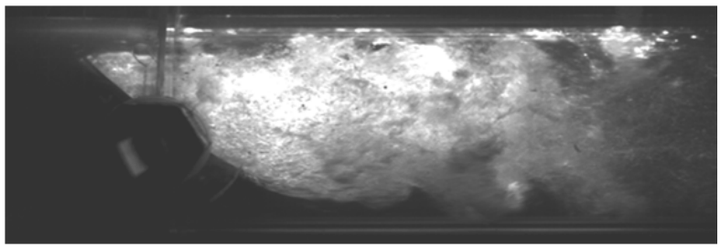

Fig. 1. Cavitation around a butterfly valve (Valve opening:45deg, Flashing Condition).

Figure 2 shows the test valves. The valve shown in Fig.2(a) is a normal valve without a fin

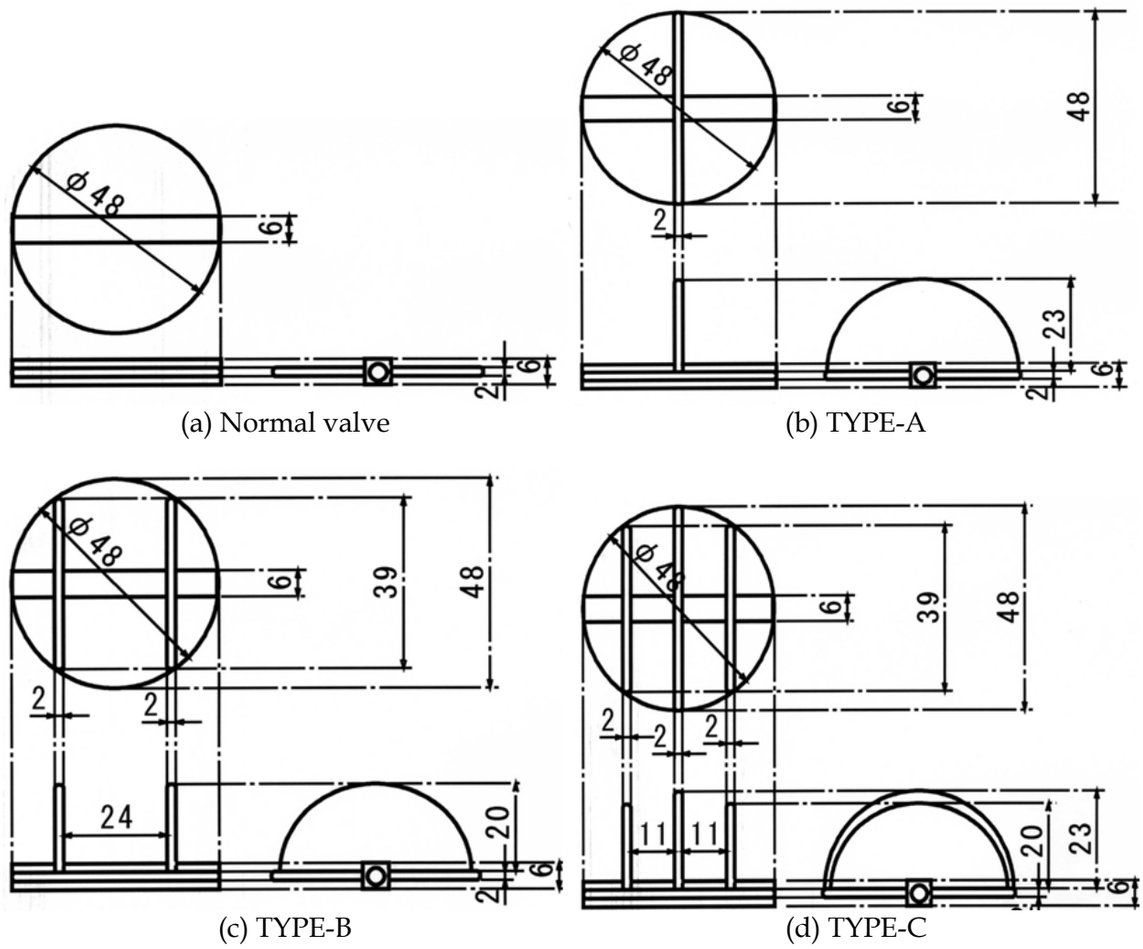

(a) Normal valve (b) TYPE-A

(c) TYPE-B (d) TYPE-C

Fig. 2. The test valves with fins.

The author clarified that the fin must be installed in the downstream of the valve in order to reduce cavitation (Ogawa & Uchida,1995). In this study, a test valve is called "TYPE-A" when a semicircular fin is attached to the downstream surface of the valve. When two semicircular fins are attached to the downstream surface of a valve, the test valve is called "TYPE-B". On the "TYPE-C" test valve, three semicircular fins are attached to the downstream surfaces of the valve. For each valve, each fin was fixed perpendicular to the valve stem.

Cavitation noise measurements were performed in a closed-type cavitation tunnel, using water as the fluid. There was a pump on the downstream side of the test section. The upstream pressure was kept at atmospheric pressure and the valve opening was fixed during the experiment. The flow velocity was increased by controlling the frequency of the pump using an inverter. Cavitation noise was measured at each flow velocity and a visualization was created by a high-speed camera. Cavitation noise was measured using a noise meter placed close to the outside surface of the test section duct. The frequency range of this noise meter was 20-8000Hz.

3. Cavitation number and pressure loss coefficient

The cavitation number σ in this study is defined as follows:

$$\sigma = \frac{p - p_v}{\rho U^2 / 2} \tag{1}$$

where is upstream pressure, is saturated vapor pressure, is density of water, and U is average upstream flow velocity. The pressure loss coefficient ζ is defined by the following formula:

$$\zeta = \frac{\Delta P}{\frac{1}{2}\rho U^2} \tag{2}$$

where ΔP is the differential pressure across the test valve.

4. Effect of the fins on cavitation noise reduction (Comparison with constant valve opening)

Kimura and Ogawa(1986) clarified using measurements of cavitation erosion and noise that the cavitation around the butterfly valve occurs most intensely when the valve is halfway open (40°-45°). Therefore, noise was measured around halfway-open valves in this study, and the degree of the cavitation reduction was investigated based on these measurement results. In the experiments, cavitation noise was measured at each flow velocity, while flow velocity was increased gradually by controlling the frequency of the pump.

Figure 3 shows the results of noise measurement when the valve was kept open constantly. The effect of the fins on noise was clear in the case of TYPE-B. In the case of the normal valve without a fin, cavitation occurred at, but in the case of TYPE-B, cavitation occurred at. These results proved that cavitation occurrence was suppressed by the fins. Moreover, the maximum noise just before flashing was 5dB lower in the case of TYPE-B than in the case of the normal valve.

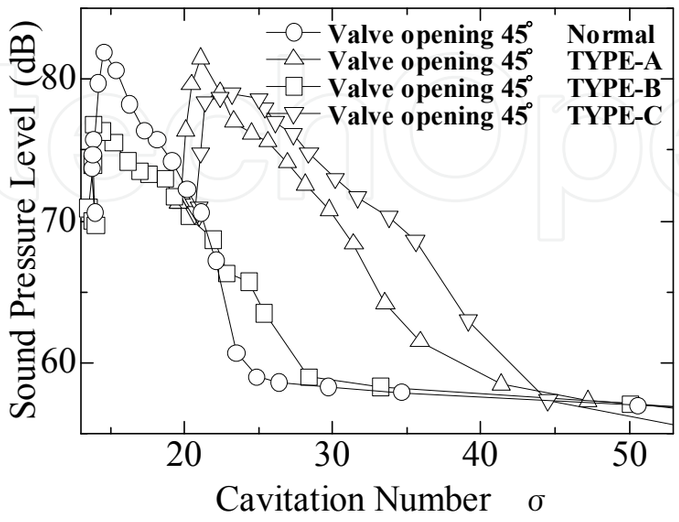

Fig. 3. Effect of Fins on Cavitation Noise (Normal,TYPE-A,B,C: Valve Opening=45deg).

In the cases of TYPE-A and TYPE-C, the cavitation number at cavitation inception was larger than that in the case of the normal valve. The fin promoted the occurrence of cavitation because the middle fin was fixed on the orifice side, where cavitation occurrence was intense.

5. Effect of the fins on cavitation noise reduction (Comparison with constant pressure loss coefficient)

The results shown in Fig. 3 were obtained by measuring cavitation noise at each flow velocity, while flow velocity was increased using a pump controlled by an inverter. The upstream pressure was kept at atmospheric pressure in each experiment, and the effect of the saturated steam pressure was minimal. Therefore, the flow velocity was also almost the same when the cavitation number was same. However, in many cases, the flow rate was not controlled by changes in the frequency of the pump, and the flow rate was controlled by adjusting the opening of the valve. Additionally, the flow rate in the actual plant was determined by the head curve of the pump and the pressure loss of the piping system as s whole. Accordingly, the effect of cavitation control should also be investigated under the constant pressure loss coefficient condition.

When a fin is attached to a valve body, the flow rate may be changed by the variation in the pressure loss of the valve. Figure 4 shows the pressure loss coefficients for each type of valve. For an example, the pressure loss of TYPE-C was larger than that of the normal valve at the same Reynolds number and at the same valve opening. When the butterfly valve is used to control the flow rate, the valve opening of TYPE-C must be larger than that of the normal valve in order to obtain the same flow rate. Therefore, the experimental results must be compared with a constant pressure loss coefficient. The following discussion is based on a comparison of cavitation noise under the condition that the pressure loss coefficients of the test valves are nearly equal.

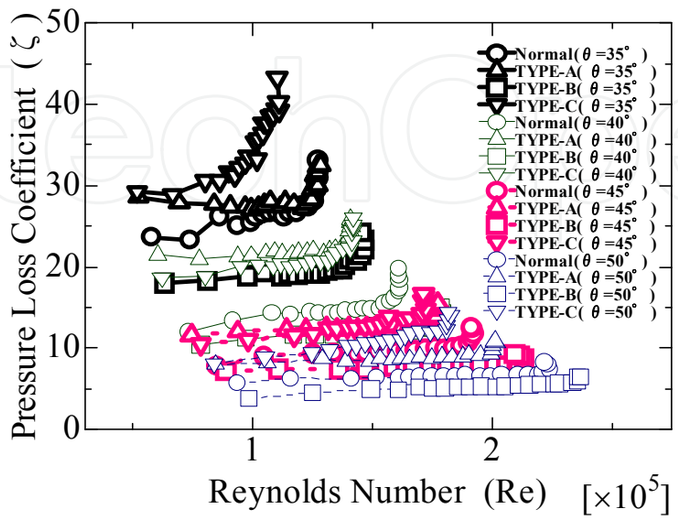

Fig. 4. Pressure Loss Coefficients for each Valve Type.

Figure 5 shows the pressure loss coefficients for each valve when σ was about 7. The pressure loss coefficient was almost constant for each valve within the range of the Reynolds number of the experiment. However, when the Reynolds number was $\mathrm{Re} = 2.25 \times 10^5$ in the case of TYPE-C, the pressure loss coefficient began to increase and the noise began to decrease corresponding to flashing. According to the results shown in Fig.5, the noise levels around each valve were compared with a pressure loss coefficient of about 7.

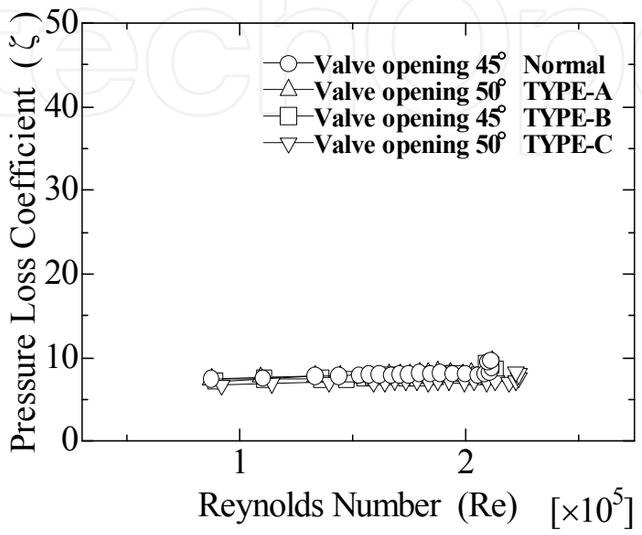

Fig. 5. Pressure Loss Coefficients (ζ≒7).

Figure 6 shows the effect of the fins on cavitation noise. The pressure loss coefficient for Type-B was about 7 at the valve opening of 45° and almost the same as that for the normal valve at the valve opening of 45°. Cavitation began to occur at about $\sigma = 30$ in the case of TYPE-B. On the contrary, in the case of the normal valve, light cavitation noise occurred

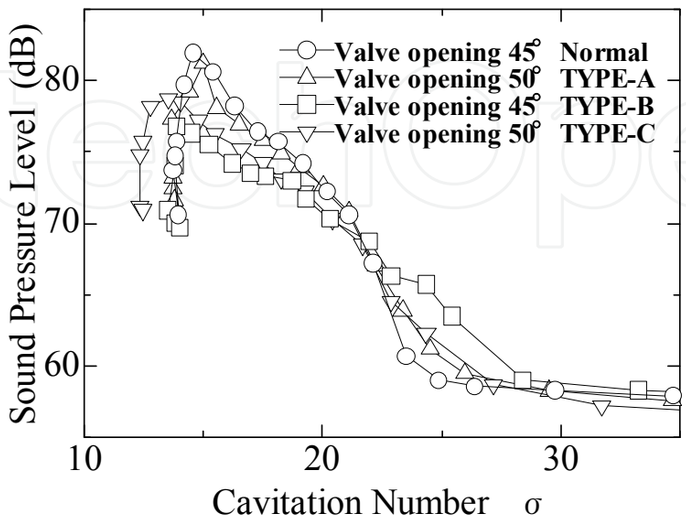

Fig. 6. Effect of Fins on Cavitation Noise under ($\zeta \fallingdotseq 7$).

around almost all the edges of the valve body at about $\sigma = 25$, where the sound pressure level of the cavitation began to rise abruptly. Accordingly, the inception of cavitation for TYPE-B was earlier than that for the normal valve. However, the results shown in Fig.6 indicate that the maximum cavitation noise value was suppressed in TYPE-B by the fins. Cavitation noise was reduced by about 5 dB when . The noise reduction effect in TYPE-B was remarkable just before flashing condition. Though cavitation occurred a little earlier than with the normal valve, the increase in the noise was milder in TYPE-B and the maximum sound pressure was suppressed.

The accuracy of the data mentioned above was ±1-1.5 dB near the inception of cavitation and ±0.5dB during cavitation growth and flashing. Though the differences among the valves were slight as shown in Fig.6, the noise reduction effect was clear for TYPE-B in flashing even taking into account the accuracy of the data.

6. The visualization of the effect of the fins

6.1 Visualization experiments

Figs. 7 and 8 show the photographs of the cavitation conditions of each valve taken with a high-speed camera. Figure 7 was taken through the upper surface of the transparent pipe (top view). Figure 8 was taken from the side surface (side view). These photographs were not taken simultaneously because only one camera was available to be used. As shown in Fig. 7(a), vortex cavitation clouds were clearly visible on the orifice side of the normal valve and 1 Dia and further downstream from the stem axis. These cavitation clouds were identified as vortices of an intensity which brings about the cavitation damage (Tani et al.,1991). Similar vortex cavitation also occurred in the TYPE-A valve with one fin. It was impossible to suppress flow interference using only a single fin. Moreover, it is obvious from Fig.7 (b) that the cavitation was further intensified since the fin existed in the part of the orifice side where the contraction flow was severe. However, such a vortex cavitation cloud is not clear around the TYPE-B valve as shown in Fig. 7(c). The interference of the flow from the orifice side with the flow from the nozzle side seemed to be suppressed by the fins. Accordingly, it can be said that the cavitation around the valve body in TYPE-B was

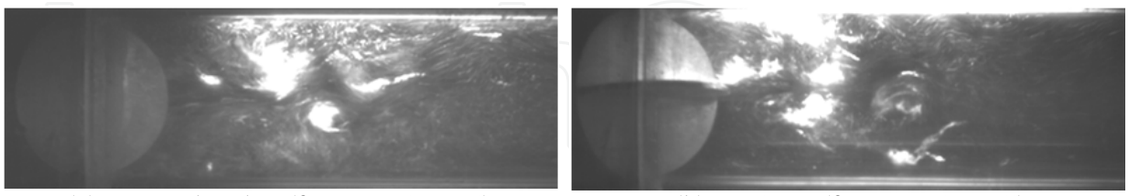

(a) Normal Valve (θ=45°,σ=17,ζ=8) (b) TYPE-A (θ=50°,σ=17,ζ=8)

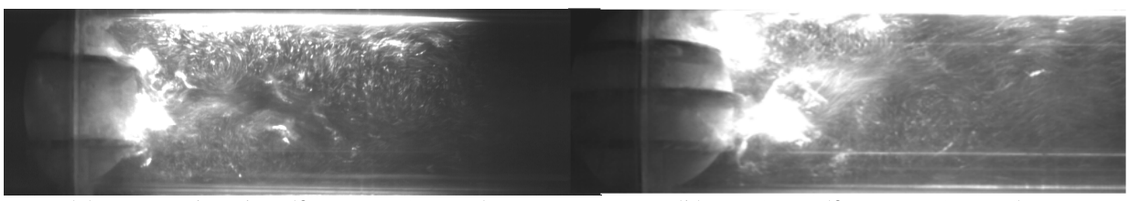

(a) Normal Valve (θ=45°,σ=17,ζ=8) (b) TYPE-A (θ=50°,σ=17,ζ=8)

Fig. 7. Top Views of Cavitation Conditions.

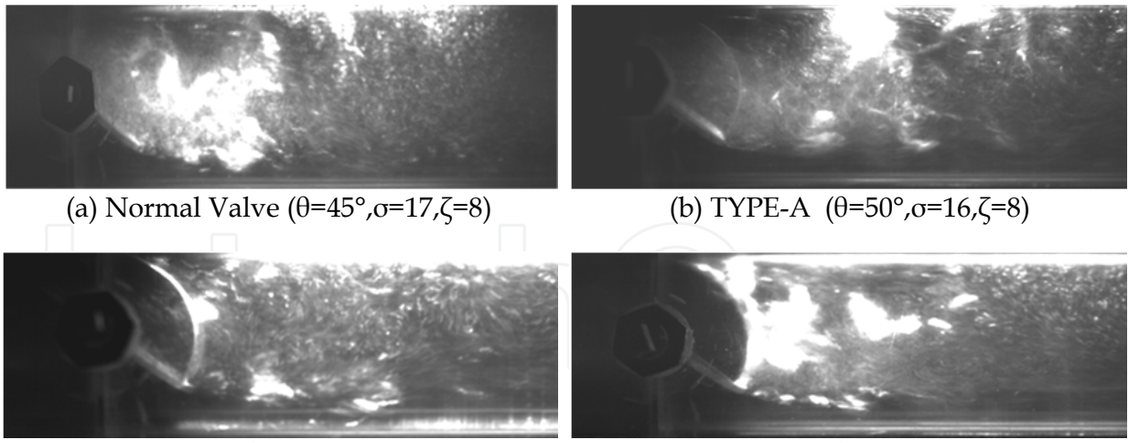

(a) Normal Valve (θ=45°,σ=17,ζ=8) (b) TYPE-A (θ=50°,σ=16,ζ=8)

(c) TYPE-B (θ=47.5°,σ=16,ζ=8) (d) TYPE-C (θ=50°,σ=16,ζ=8)

Fig. 8. Side Views of Cavitation Conditions.

suppressed by the attachment of the fins. As for the TYPE-C valve with three fins, though the two fins on either side of the valve probably suppressed the cavitation as they did for the TYPE-B valve, it is appropriate to conclude from Fig.7(d) that the cavitation reduction effect was not obtained because the central fin intensified the cavitation as it did for the TYPE-A valve.

The photograph in Fig.8(c) shows that cavitation was moderate for TYPE-B in comparison to the other three valve types. In TYPE-A and TYPE-B, in the vicinity of the upper wall of the position 1 Dia from the valve stem, vortex cavitation was remarkable as mentioned above.

6.2 Numerical simulation

Numerical analysis was carried out in order to examine the effects of the fin. The numerical analysis code was Star-CD and the barotropic model was used as a model for cavitation. The calculation conditions were $\theta = 45°$ and $\sigma = 22$. Figure 9 shows the calculation results of calculating velocity vectors and Figure 10 shows the coordinate system according to numerical analysis. The origin is at the center of the valve stem. Velocity vectors were examined in the cross section which is near the fin in order to clarify the effects of the fin. Figs.9 (a),(c),and (e) show the velocity vectors for the cross-section which was at Y=15mm (Y=0.3Dia.). Figs.9 (b),(d),and (f) show the velocity vectors for the cross section which was at X=15mm (X=0.3Dia.). The fin is not shown in figures (b),(d), or (f) because the fin is not part of the cross section in the position where X=0.3 Dia.

Fig.9(a) reveals that for the normal valve, the flow from the orifice side and the flow from the nozzle side interfered with one another about 1 Dia from the valve stem. This interference made the downstream flow of the valve swell and brought about intense vortices. These vortices is correspond to the cloud cavitation shown in Fig.7(a).

The swell of the flow for the TYPE-B valve with two fins was relatively moderate in comparison with that of the normal valve. It is clear from Fig.9(c) that the swell of the flow is the smallest for the TYPE-C valve. However, it is probable that the cavitation intensified since the fin was located in a position where the contraction flow was severe. Fig.9 (f) shows a contraction flow more severe than that of the other valves on the orifice side. Accordingly,

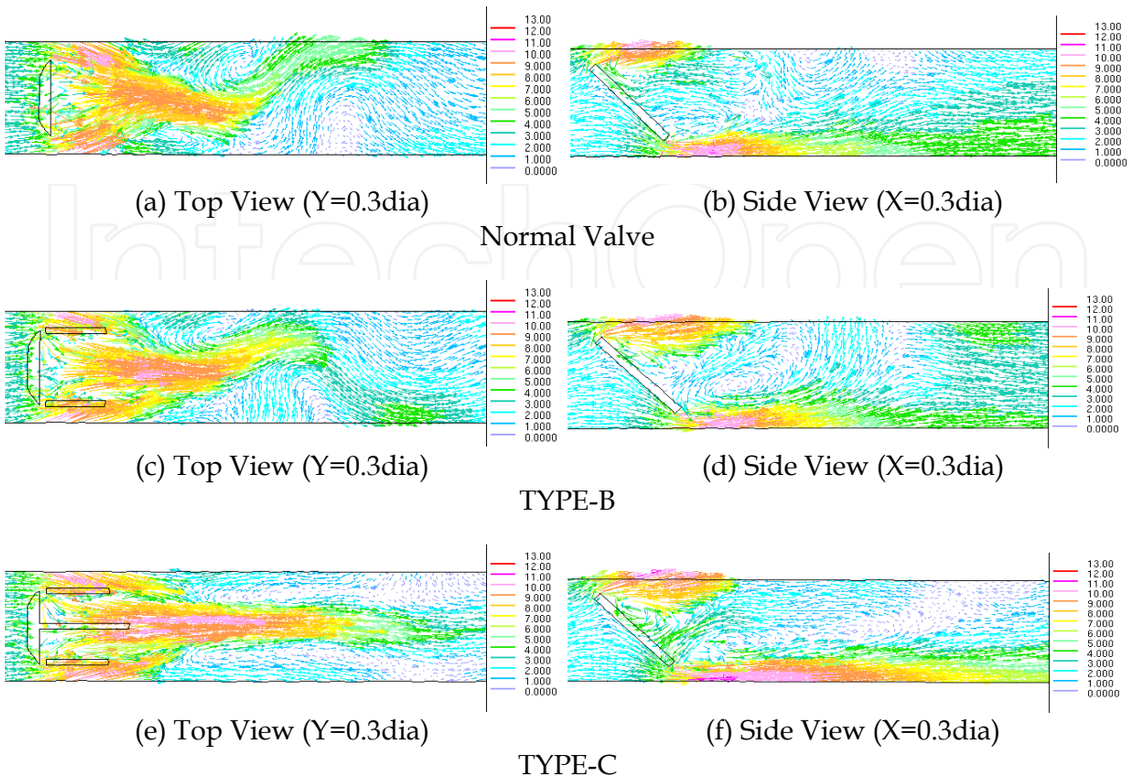

Fig. 9. Cavitation Flow around a Butterfly Valve (θ=45°,σ=22).

in TYPE-C, the flow interference effect was suppressed by the two fins on either side of the valve, but was canceled out by the intensification of cavitation due to the central fin. Therefore, the effect wherein two fins on either side of a valve suppresses flow interference is offset by the effect wherein the fin in the center intensifies cavitation.

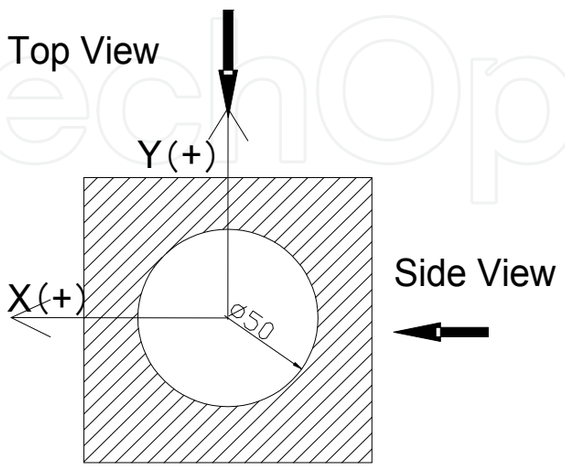

Fig. 10. Coordinate System in Numerical Analysis.

7. The effect of the upstream velocity distribution on butterfly valve cavitation

7.1 Velocity distribution

A straight length in front of a butterfly valve is needed to obtain a normal velocity distribution as shown in Fig.11(a). In a turbulent flow, the entrance length to obtain fully developed flow is about fifty or one hundred times the pipe diameter. However in practical engineering, more than two valves are installed in series or bends are installed just ahead of a valve to save space. Under such conditions, the upstream velocity distribution is very different from the normal turbulent velocity distribution. In this study, the cavitation noise measurement was performed under such a velocity distribution that there was a large velocity difference between the nozzle side and the orifice side.

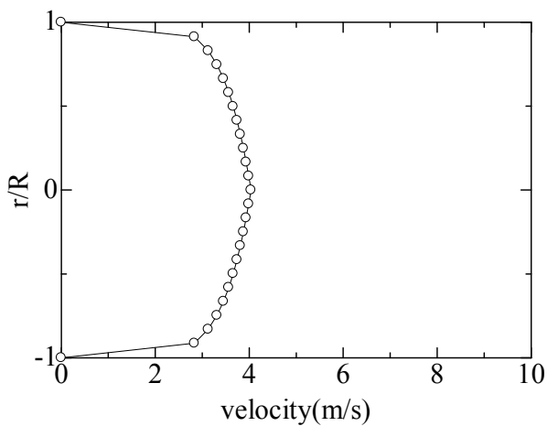

(a) Normal velocity distribution

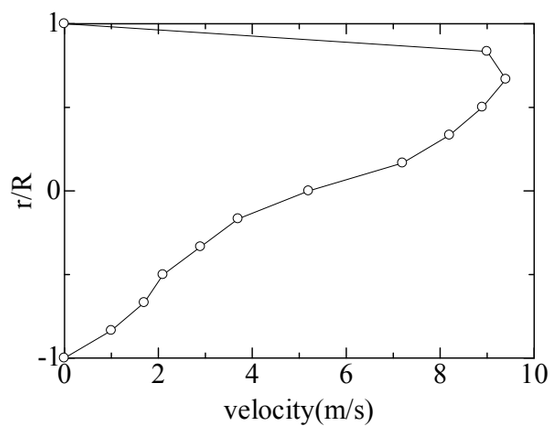

(b) Biased velocity distribution (A)
(The orifice side velocity is larger than the nozzle side velocity.)

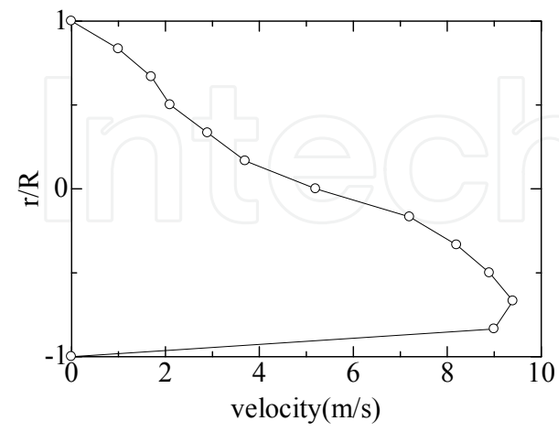

(c) Biased Velocity distribution (B)

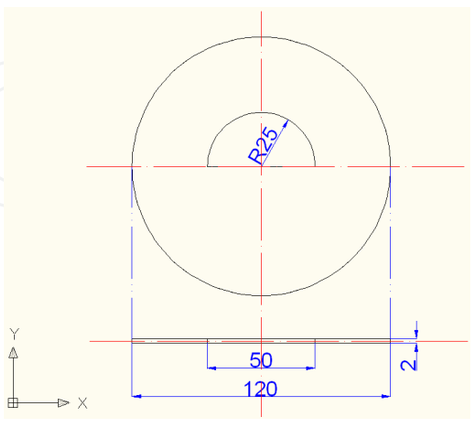

(d) The Circular Plate for biased velocity
(The nozzle side velocity is larger than distribution the orifice side velocity.)

Fig. 11. Velocity distribution upstream of the butterfly valve and the Circular Plate for biased velocity.

A plate with a half circle hole shown in Fig.11(d) was installed at 3D (D: pipe diameter) upstream of the valve to obtain an biased velocity distribution. The velocity distributions were analyzed by numerical simulation using a commercial code Star-CD because the measurement of the velocity distribution was difficult behind such plate. Fig.11 shows three types of velocity distributions. The vertical axis shows the location divided by the radius of the pipe and the horizontal axis shows velocity. Fig.11 (a) shows an example of a normal turbulent velocity distribution at 1D upstream of the valve. Fig.11 (b) and Fig.11 (c) show the biased velocity distributions. In each example, the average velocity was $3m/s$. In Fig.11 (a), the velocity distribution mostly agreed with Blasius's law. In Fig.11(b), the velocity on the orifice side of the valve was larger than that on the nozzle side of the valve. The velocity distribution of Fig.11(c) is the reverse of Fig.11 (b).

In many practical industry plants, the flow rates are controlled by adjusting the opening of the butterfly valve and are determined by head curves of pumps and pressure losses of the whole piping systems. Accordingly, the effect of valve shape on cavitation noise should also be investigated under the condition of a constant pressure loss coefficient.

In the flow of the normal velocity distribution, the cavitation at the orifice side becomes severe since the contraction at the orifice side becomes intense and the pressure around the edge becomes very low. As shown in Fig.12, the cavitation inception of the Type-B valve was observed at $\sigma = 38$, but in contrast the cavitation inception of the normal valve was observed at $\sigma = 58$. Moreover, the increase of cavitation noise of the Type-B valve was suppressed after inception. As for the maximum noise, the Type-B valve was lower than the normal valve. Therefore, the effect of semi-circular fins is clear.

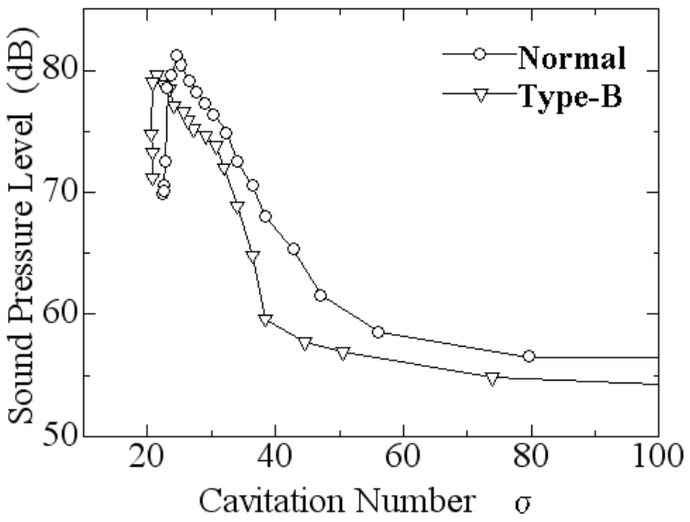

Fig. 12. Cavitation Noise under normal velocity distribution ($\theta = 45°$, $\varsigma = 12$).

Figure 13(a) shows the cavitation noise in the flow of the biased velocity distribution (A). In this case, the flow rate of the orifice side was much larger than that in the normal velocity distribution. Accordingly, the cavitation noise of both the normal valve and Type-B valve were increased remarkably in the range of $\sigma = 30$ to $\sigma = 50$ compared with the results of

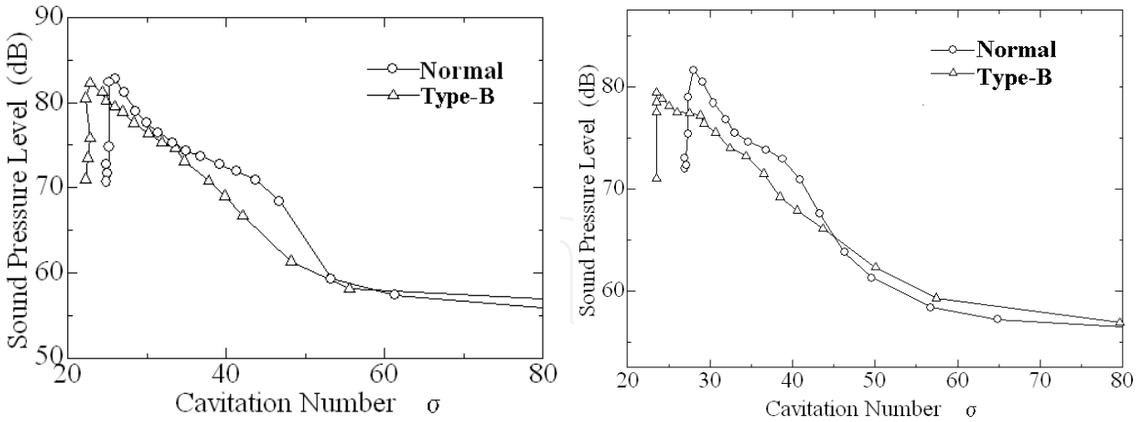

(a) Cavitation Noise under biased velocity distribution (A) ($\theta = 50°$, $\varsigma = 17$)

(b) Cavitation Noise under biased velocity distribution ($\theta = 50°$, $\varsigma = 13$)

Fig. 13. Cavitation Noise under biased velocity distribution.

Fig.12. However, the noise of the Type-B was smaller than that of the normal valve. The effect of the fins remained in the biased velocity distribution.

Figure 13(b) shows the cavitation noise in the flow of the biased velocity distribution (B). In this case, the cavitation noise was relatively smaller than that in the biased velocity distribution (A), but much larger than that in the normal distribution. However, the noise of the Type-B was smaller than that of the normal valve. Therefore, it is clear that the effect of the semi-circular fins holds even in the biased velocity distribution and that the cavitation noise is larger when the velocity distribution is biased.

7.2 Diameters and numbers of cavitation bubbles around the butterfly valves

7.2.1 Cavitation condition

Fig.14 shows the cavitation conditions of the normal valve. These photographs were taken under the condition that the acrylic tube for visualization was illuminated by a metal halide light source and with a zoom lens and a bellows were attached to the high speed camera. The upper photographs show the whole of the butterfly valve cavitation, and the lower photographs show individual cavitation bubbles. The flow direction is from left to right. The lower photographs were taken at the position of 1.5 dia to the downstream direction from the butterfly valve center. The size of the visual field had a length of 1.3mm, and width of 6mm.

Under the inception condition shown in Fig 14(a), some bubbles were observed. There is a large bubble in the upper left, however the number of cavitation bubbles is little, and the diameter is also small.

Under the growth condition in Fig.14(b), the cavitation region extends to the 1.5dia downstream and the number of cavitation bubbles increase remarkably. Cavitation bubbles with diameters are from $20\mu m$ to $200\mu m$ were observed.

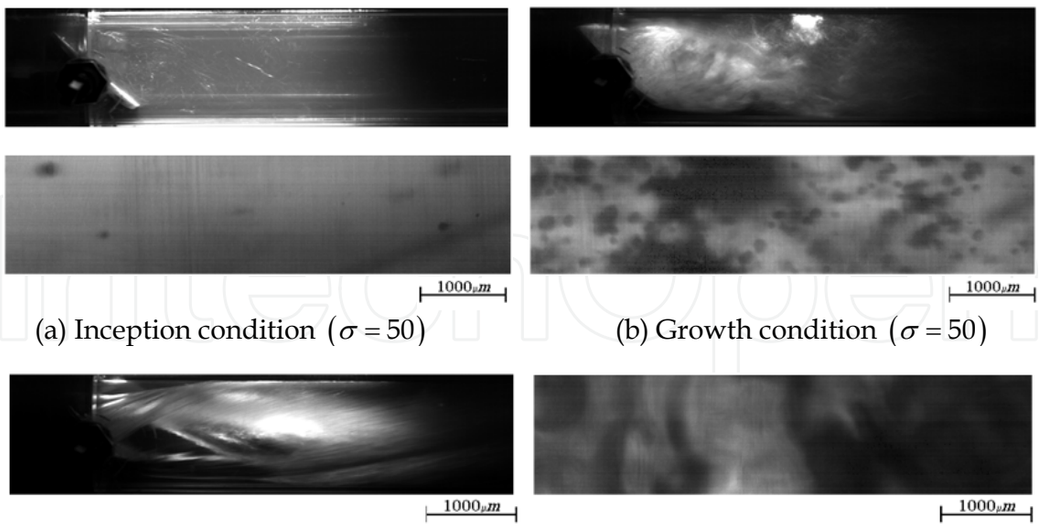

(a) Inception condition $(\sigma = 50)$ (b) Growth condition $(\sigma = 50)$

(c) Flashing condition $(\sigma = 50)$

Fig. 14. Cavitation Bubbles of the normal valve ($\theta = 45°$).

Under the flashing condition as shown in Fig.14(c), a large cavity was formed behind the valve, therefore the individual cavitation bubbles were not be able to be photographed except for the near wall.

7.2.2 Diameters and numbers of cavitation bubbles

Fig.15 shows the diameters and numbers of cavitation bubbles of the normal valve under the normal velocity distribution. The diameter of the bubbles are shown at 8 stages at every $30\mu m$. For example, a bubble with a diameter between 20 μm and 50 μm is expressed as 35 μm , and a bubble with a diameter between 50 μm and 80 μm is expressed as 65 μm . Bubbles with diameters were smaller than 20 μm could not be visualized in our experiments. Such size nuclei are presumed to be contained even in water under non-cavitation conditions, and will not affect cavitation noise greatly. The bubbles with diameters larger than 230 μm did not occur in our experiments. In Fig.14, the cavitation condition reached the flashing condition at $\sigma = 24.2$. As for the flashing condition, the number of bubbles is shown as zero because the individual cavitation bubbles were not able to be photographed.

The inception condition was at $\sigma = 48$ and the flashing condition was at $\sigma = 25$. Under the normal velocity distribution, the diameters ranged mainly from 20 μm to 100 μm as shown in Fig.15(a). However, under the biased velocity distribution (A), the cavitation bubbles with diameters over 100 μm increased at $\sigma = 35.9$ as shown in Fig.15(b). Under this condition, the cavitation condition was in the growth stage and the cavitation bubbles occurred numerously behind the valve body. Though it looks as if the amount of the bubbles decreased compared with Fig.8, this is due to the fact that the photographing was performed at one position. Compared with the results of Fig.15(a), the cavitation noise in Fig.15(b) had already become more intense at the same cavitation number.

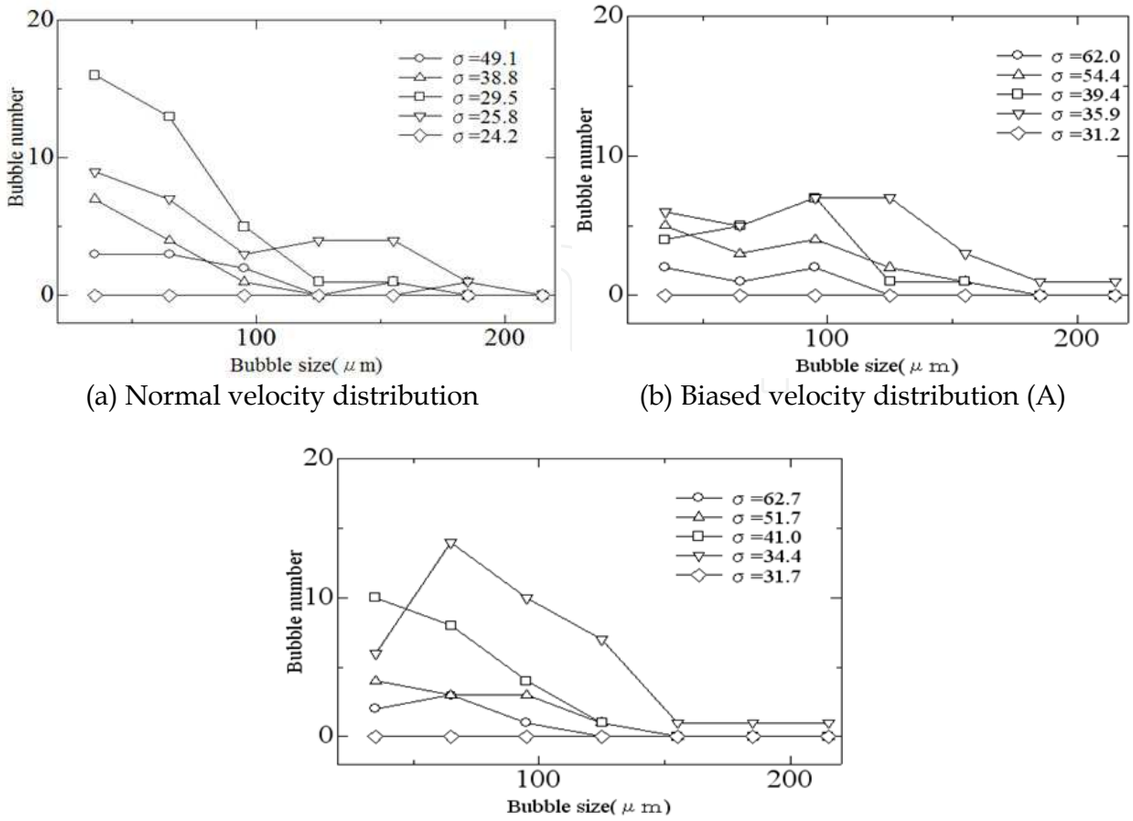

(a) Normal velocity distribution (b) Biased velocity distribution (A)

(c) Biased velocity distribution (B)

Fig. 15. Diameters and numbers of cavitation bubbles of the normal valve ($\theta = 45°$).

Fig.15(c) shows the diameters and numbers of cavitation bubbles under the biased velocity distribution (B). At $\sigma = 34.4$, the numbers of the cavitation bubbles with diameters between 65 μm and 125 μm increased remarkably comparing with the results of Fig.15(a). From the results of Fig.15(a),(b) and (c), when the bubbles with diameters from 20m to 30m increased, the cavitation noise tends to increase.

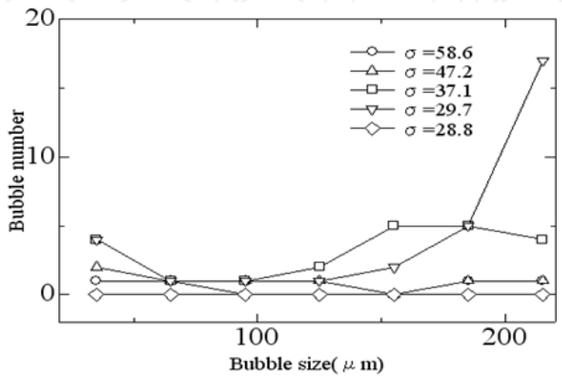

Fig. 16. Diameters and numbers of cavitation bubbles of the Type-B valve under the normal velocity distribution ($\theta = 45°$).

In the case of Type-B as shown in Fig.16, the cavitation numbers were less than the case of the normal valve. Though the cavitation bubbles with diameters larger than $200\,\mu m$ increased greatly at $\sigma = 29.7$, this condition was just before the flashing and the number of bubbles was suppressed compared with the case of the normal valve in the range of diameters from $35\mu m$ to $125\mu m$.

7.3 The aspect of cavitation bubbles

Figure 17 and Table 1 shows the positions of photographing. Position A was very near the leading edge of the valve body. Position B was in the wake region of the valve. Position C was on the centerline of the pipe and near the end of the cavitation clouds.

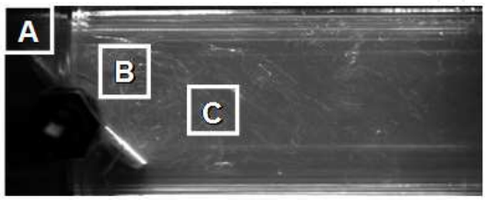

Fig. 17. The details of Photographing positions.

Position	x	y	Photographed Area a×b(mm)	Frame (per second)
A	-0.2 dia.	0.36 dia.	0.6×5.0	20000
B	0.3 dia.	0.3 dia.	1.7×6.8	10000
C	1.3 dia.	0 dia.	1.7×6.8	10000

Table 1. Photographing Positions.

Fig.18 shows the occurrence of the cavitation bubbles at position A. The five photographs in the image were of a series and photographed at 20000 frames/second. Position A was near the leading edge and the crescent in the central lower of the photograph is the one part of the leading edge of the valve body. It is very clear that the cavitation bubble occurred at the position on the right in the leading edge when photograph (c) is compared with photograph (d). The bubble seems to be oval and the size is about 200 μm . The cavitation bubble grows larger in the left side of the photograph.

Fig.19 shows the cavitation bubbles at position B. Oosition B was 0.3dia. downstream of the valve. This position is in the large separation region behind the valve. Though the mainstream is the right direction from the left, the flow circulates in the separation region, and the bubbles of the photograph move from the right to the left. The diameters of the bubbles range from 20μm to 200μm .

Fig.20 shows the cavitation bubbles at position C. Position C was 1.3dia. downstream of the valve. In this figure, the bubbles move from left to right and the number of the bubbles were relatively larger than that at position B. This vicinity is the position where the cavitation cloud ends, and the number of bubbles increases because the bubbles which have been flowing from the orifice and nozzle side flow together.

(a) t=1/20000(s)

(b) t=2/20000(s)

(c) t=3/20000(s)

(d) t=4/20000(s)

(e) t=5/20000(s)

Fig. 18. Cavitation Bubbles at the Position A (valve opening= 45° , $\sigma = 48.6$).

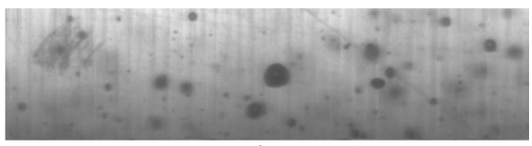

(a) t=1/10000(s)

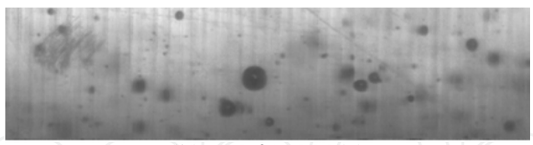

(b) t=2/10000(s)

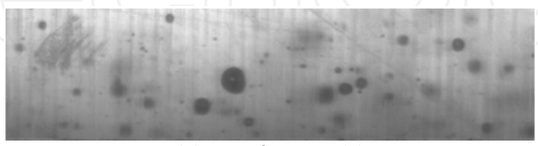

(c) t=3/10000(s)

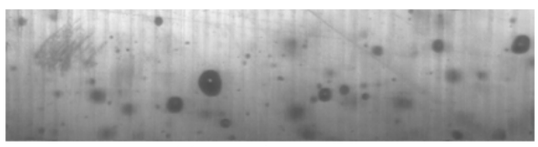

(d) t=4/10000(s)

Fig. 19. Cavitation Bubbles at the Position B (valve opening= 45° , $\sigma = 51.7$).

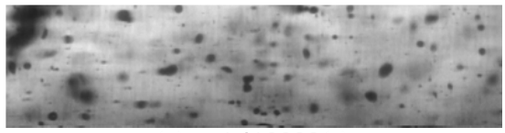

(a) t=1/10000(s)

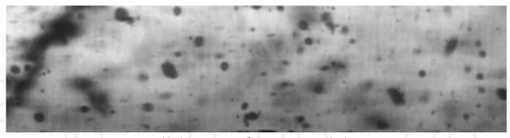

(b) t=2/10000(s)

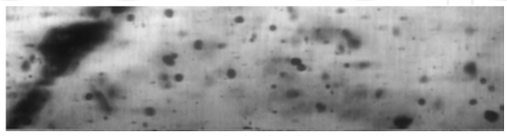

(c) t=3/10000(s)

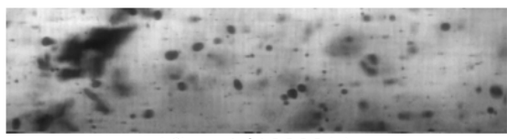

(d) t=4/10000(s)

Fig. 20. Cavitation Bubbles at the Position C (valve opening= 45° , $\sigma = 44.6$).

8. Conclusions

The ability of fins to reduce the cavitation noise around a butterfly valve was investigated in this study. When two semicircular fins were attached to the downstream side of a valve body (TYPE-B), the experimental results indicated that the inception of cavitation was earlier than that found with a normal valve. This was discovered via comparison of noise given a constant pressure loss coefficient. However, cavitation noise increased gradually after inception and the maximum value of cavitation noise just before flashing was shown to be suppressed for the TYPE-B valve by the fins. Cavitation noise was reduced by about 5 dB when a valve opening of 45degrees was used. The effect of noise reduction around the TYPE-B valve was most remarkable just before flashing. In this study, it was found that fins are an adequate method for the reduction of cavitation noise. The optimum size and position of the fins should be investigated in future studies.

Visualizations created by a high-speed camera showed that intense vortex cavitation clouds were not clear in the TYPE-B valve with two fins. The interference of the flow from the orifice side with the flow from the nozzle side seemed to be suppressed by the fins. This was also confirmed by numerical analysis.

As for the visualization of cavaitation bubbles by using high-speed camera, it was found in this study that cavitation bubbles occur at the position before the leading edge and that the cavitation bubbles grow larger just behind the leading edge. It was also found that the maximum diameter occurs near the leading edge and that the bubbles become smaller through the pressure recovery of the flow. In this observation, the maximum diameter of the bubbles was 500μm near the leading edge. The diameter of the bubbles ranged from 20μm

to 200μm at position B and position C. It is considered that the cavitation occurrence is dominant at the leading edge by the contraction flow and that the bubbles which occur at the leading edge become smaller in size through pressure recovery.

As for the effect of velocity distribution, it was clarified in this study that the cavitation noise around a butterfly valve becomes larger when the upstream velocity distribution was different from the normal velocity distribution. It was clear that the interference of the flow from the orifice side and the flow from the nozzle side was suppressed by the fins under not only the normal velocity distribution but also under the biased velocity distribution. The cavitation noise of Type-B was smaller than that of the normal valve in each upstream velocity distribution. Moreover, from the visualization results, it was found that the cavitation bubble diameters ranged from about 20 μm to about 200 μm and that the numbers of cavitation bubbles in Type-B was less than that of the normal valve.

9. References

Baumann, H.D.,(1991), *Control Valve Primer*, Instrument Society of America, pp.100-107.

Itoh, Y., Yamada,M., Oba, R. et al., (1988). *A peculiar Behavior of Cavitating Flow around a Butterfly Valve*, Transactions of the Japan Society of Mechanical Engineers, Series B, Vol.54, No.508, pp.3317-3224.

Kimura,T. and Ogawa,K., (1986), *Cavitation Vibration and Noise around a Butterfly Valve*, Vol.25, No.1, ISA Transactions, p.53-61.

Kimura,T. and Ogawa,K.,(1997), *Measurement of Cvaitation Erosion Using Fragile Material*, Transactions of the Japan Society of Mechanical Engineers, Series B, Vol.63, No.606, pp.360-365.

Kugou, N., Matsuda, H. et al.,(1996), *Cavitation Characteristics of Restriction Orifices (Experiment on Characteristics of Piping Vibration and Noise*, Fluids Engineering Conference, Volume 1, ASME FED-Vol.236, pp.457-462.

Ogawa,K. and Uchida,T., (2005), *Noise reduction of a butterfly valve cavitation by fins and improvement of shape of a piping arrangement*, ISA 2005 Technical Conference, (2005), ISA05-P179.

Ogawa,K., (2008), *Noise Reduction in Butterfly Valve Cavitation by Semicircular Fins and Visualization of Cavitation Flow*, 54th International Instrumentation Symposium,IIS-P047.

Rahmeyer,W.J.,Miller, H.L. and Sherikar, S.V.,(1995), *Cavitation Testing Results for a Tortuous Path Control Valve*, Cavitation and Multiphase Flow, ASME, FED-Vol.210, (1995), pp.63-67.

Tani, K., Ito,.Y, and Oba, R., (1991), *Spatial Distributions of Cavitaion Induced Pressure-Pulses around a Butterfly Valve*, Cavitation and Multiphase Flow Forum, ASME, FED-Vol.109,pp.143-147.

Tullis, J.P., (1989). *Hydraulics of Pipelines -Pumps, Valves, Cavitation, Transients-*, John Willey & Sons, pp.125-126.

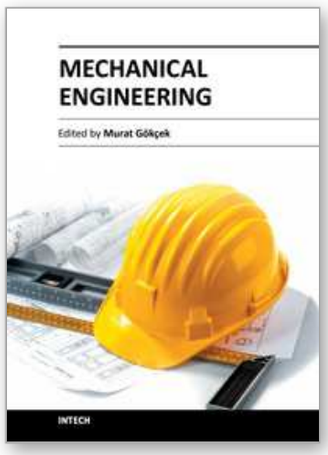

Mechanical Engineering

Edited by Dr. Murat Gokcek

ISBN 978-953-51-0505-3
Hard cover, 670 pages
Publisher InTech
Published online 11, April, 2012
Published in print edition April, 2012

The book substantially offers the latest progresses about the important topics of the "Mechanical Engineering" to readers. It includes twenty-eight excellent studies prepared using state-of-art methodologies by professional researchers from different countries. The sections in the book comprise of the following titles: power transmission system, manufacturing processes and system analysis, thermo-fluid systems, simulations and computer applications, and new approaches in mechanical engineering education and organization systems.

InTech Europe
University Campus STeP Ri
Slavka Krautzeka 83/A
51000 Rijeka, Croatia
Phone: +385 (51) 770 447
Fax: +385 (51) 686 166
www.intechopen.com

InTech China
Unit 405, Office Block, Hotel Equatorial Shanghai
No.65, Yan An Road (West), Shanghai, 200040, China
中国上海市延安西路65号上海国际贵都大饭店办公楼405单元
Phone: +86-21-62489820
Fax: +86-21-62489821

IntechOpen